# Recovery Is Not Return to Baseline: Coherence Operators for Measuring Biological Recovery Signatures

Joel Thorarinson* Allison Hensgen† Iulia Koplik‡

June 2026

**Abstract**

A patient's resting heart rate returns to 72 bpm after surgery. Blood pressure normalizes. Lab values fall within reference ranges. Three months later, they present with heart failure. The problem is not the measurements — it is what they fail to measure. Threshold-based clinical assessment treats recovery as return to baseline values, but a system can recover its resting statistics while its capacity for *coherent recovery* — the ability to respond to perturbation consistently, efficiently, and adaptively — has degraded. We propose a translational framework that brings validated engineering coherence operators into biological measurement through six operationally defined recovery signatures: baseline deviation, post-perturbation persistence, recovery half-life, variability stabilization, episode repeatability, and adaptive response quality. Each signature is formalized using operators from the Coherence Engine [Thorarinson and Hensgen, 2026a], adapted to the specific characteristics of biological data: high noise, individual variation, compensatory dynamics, and non-stationarity. We ground the framework in experimental biophoton literature demonstrating that coherence transitions are directly measurable in living systems [Benfatto et al., 2021, Wang et al., 2023], and apply it to five domains — cardiac, metabolic, neurological, immune, and sleep — with one testable prediction per domain. We describe a practical pipeline for computing recovery signatures from consumer wearable data and publicly available PhysioNet datasets (MIT-BIH Arrhythmia Database, CHB-MIT Scalp EEG Database). The central distinction is between *true recovery* and *compensation*: two systems with identical resting values can have measurably different recovery dynamics, and this difference is where early warning of functional decline lives.

**Keywords:** biological coherence; recovery signatures; critical slowing down; wearable data; heart rate variability; continuous glucose monitoring; early warning; adaptive response

## 1 Introduction

A patient recovers from surgery. Their resting heart rate returns to pre-operative levels within a week. Their blood pressure normalizes. Their laboratory values fall within reference ranges. By every conventional metric, they have recovered. Yet three months later, they present with heart failure.

This scenario is not hypothetical. It reflects a fundamental limitation of threshold-based clinical assessment: the assumption that return to baseline statistics constitutes recovery. A system can return to its baseline *values* while its baseline *dynamics* have degraded. The resting heart rate may be 72 bpm, but the beat-to-beat variability — the signature of a healthy, adaptable autonomic nervous system [Task Force of the European Society of Cardiology and the North

*Coherence Research Group. ORCID: 0000-0002-0553-842X. joel.thorarinson@conformalmaps.com
†Coherence Research Group. ORCID: 0009-0008-7247-0307
‡Coherence Research Group. ORCID: 0009-0005-3765-4811

American Society of Pacing and Electrophysiology, 1996, Shaffer and Ginsberg, 2017] — may have collapsed. The mean is the same; the coherence is not.

This loss of physiological complexity in the presence of apparently normal mean values was first identified by Lipsitz and Goldberger [1992] and has since been documented across organ systems [Goldberger et al., 2002, West, 2006]. Subsequent work has quantified specific aspects of this degradation: Costa et al. [2002, 2005] demonstrated through multiscale entropy (MSE) analysis that healthy physiological dynamics exhibit higher complexity than pathological ones at coarse time scales; Peng et al. [1995] showed through detrended fluctuation analysis (DFA) that healthy heart rate time series exhibit long-range correlations ($\alpha \approx 1.0$) that are destroyed by disease; and Scheffer et al. [2009] identified critical slowing down — increasing recovery time before a transition — as a universal early warning signal.

### 1.1 What This Paper Adds

These existing measures each capture one dimension of physiological degradation: MSE measures complexity loss, DFA measures correlation structure change, and critical slowing down measures recovery speed. Our framework makes three contributions beyond this prior work:

1. **Unified operator formalism.** Rather than treating complexity loss, correlation change, and recovery slowing as separate phenomena requiring separate analyses, we formalize six recovery signatures through a common mathematical framework — the Coherence Engine operators [Thorarinson and Hensgen, 2026a] — enabling joint analysis and cross-domain comparison.

2. **The recovery–compensation distinction.** We formalize the difference between *true recovery* (all six signatures return to baseline) and *compensation* (output values normalize while recovery dynamics remain degraded). Existing measures can detect degradation but do not provide a principled criterion for distinguishing these two states.

3. **Translational bridge.** The Coherence Engine operators have been validated on engineered systems where ground truth is available (turbofan degradation, industrial process drift). We propose and motivate their adaptation to biological measurement, where the same mathematical structure applies but the interpretation changes: a degrading engine cannot compensate, but a degrading biological system can — and does.

### 1.2 Biological Grounding: Biophoton Evidence

The framework requires that coherence transitions be measurable in living systems. Recent experimental work on biophoton emission provides direct evidence that they are. Benfatto et al. [2021] applied Diffusion Entropy Analysis (DEA) to photon time series from germinating lentil seeds and demonstrated anomalous scaling — a departure from the ordinary scaling index $\eta = 0.5$ — throughout the germination process. Early germination is dominated by non-ergodic crucial events (criticality-driven intermittence), while later stages transition to fractional Brownian motion with stationary infinite memory. This transition from critical to coherent dynamics is the kind of biological recovery signature our framework is designed to detect. Follow-up experiments comparing lentil and bean germination confirmed similar coherence signatures across organisms [Benfatto et al., 2023]. Brouder and Cifra [2015] provide a comprehensive review of ultra-weak photon emission (UPE) statistical properties, covering both quantum and classical coherence models and establishing measurement foundations for coherence-based biological assessment.

These biophoton studies demonstrate the *measurability* of biological coherence transitions. Our framework provides the *operational definitions* needed to turn such measurements into clinically interpretable recovery signatures.

### 1.3 The Biological Challenge

Applying coherence operators to biology is non-trivial because biological systems differ from engineered systems in four respects. They are noisier. They exhibit greater individual variation. They compensate for dysfunction through redundant pathways. And they are non-stationary — a healthy biological system *should* change over time in response to circadian rhythms, seasonal variation, aging, and adaptation. Distinguishing pathological drift from healthy adaptation requires a framework that measures not just change, but the *quality* of change. The allostatic load framework of McEwen [1998] provides the physiological basis: stress mediators are protective in the short term but damaging when the system's capacity for recovery degrades. The concept of allostatic overload [McEwen, 2004] formalizes the transition from adaptive to maladaptive responses that manifests as measurable changes in recovery dynamics.

We propose biological recovery signatures as the measurable targets for coherence-based health assessment. The framework does not replace clinical diagnosis; it provides a continuous, quantitative layer beneath the binary thresholds of conventional assessment — a layer that measures the system's capacity for coherent function, not just its current output values.

### 1.4 Paper Organization

Section 2 defines the six recovery signatures with mathematical formulations. Section 3 formalizes the recovery–compensation distinction. Section 4 applies the framework to five biological domains, each with a specific testable prediction. Section 5 describes a practical wearable data pipeline. Section 6 proposes perturbation study designs. Section 7 addresses limitations.

## 2 Biological Recovery Signatures

We define six recovery signatures that characterize how a biological system responds to perturbation and returns to coherent function. Each signature is a continuous measure, not a binary threshold, and each is computable from time-series data available from standard physiological monitoring.

### 2.1 Baseline Deviation

Baseline deviation measures the distance between the system's current operating point and its historical baseline, accounting for the natural manifold of healthy variation.

**Definition 1** (Baseline Deviation)**.** *For a physiological time series $\mathbf{x}(t) \in \mathbb{R}^n$ with historical baseline distribution $p_0$, the baseline deviation is:*

$$BD(t) = d_{FR}(p_0, p_t) = \sqrt{\int g_{ij}(\theta)\, d\theta^i\, d\theta^j} \tag{1}$$

*where $d_{FR}$ is the Fisher-Rao geodesic distance [Rao, 1945, Amari, 2016] between the baseline distribution $p_0$ and the current window distribution $p_t$, and $g_{ij}$ is the Fisher information metric.*

The Fisher-Rao distance is preferred over simpler measures (Euclidean distance between means, KL divergence) because it respects the geometry of the statistical manifold. A shift in mean heart rate from 70 to 75 bpm is statistically different from a shift from 70 to 75 bpm with doubled variance; Fisher-Rao captures both. This is the biological adaptation of the Drift operator $D(t)$ from the Coherence Engine [Thorarinson and Hensgen, 2026a]. Detrended fluctuation analysis [Peng et al., 1995] provides a complementary baseline deviation measure: deviation of scaling exponents from their baseline values is itself informative. For short or noisy biological time series, the fractional Brownian bridge methods of Dlask et al. [2019] provide robust Hurst exponent estimation applicable to baseline deviation computation.

### 2.2 Post-Perturbation Persistence

Persistence measures how long the effects of a perturbation remain detectable in the system's dynamics after the perturbation ends.

**Definition 2** (Post-Perturbation Persistence)**.** *After a perturbation ending at time $t_{end}$, the persistence is:*

$$PP(t_{end}) = \min\{\tau : BD(t_{end} + \tau) \leq \alpha \cdot BD(t_{end})\} \tag{2}$$

*where $\alpha \in (0, 1)$ is a resolution threshold (typically $\alpha = 0.1$, requiring 90% return toward baseline). If the system never returns within the observation window, $PP = \infty$.*

Increasing persistence across successive perturbation episodes is a hallmark of degrading recovery capacity. A healthy runner's heart rate variability returns to baseline within 2 hours of exercise; an overtrained runner's HRV may take 12 hours or longer. The perturbation (exercise) is the same; the persistence has changed.

### 2.3 Recovery Half-Life

Recovery half-life measures the timescale on which the system returns halfway to its baseline state — the biological analog of critical slowing down [Scheffer et al., 2009, Dakos et al., 2012, Lenton, 2011]. The Coherence Engine defines a Windowed Recovery operator $W(t)$ that measures whether perturbations contract or grow over a fixed time horizon [Thorarinson and Hensgen, 2026a, Definition 3]. We adapt this for biological measurement by instead tracking the time required to reach the half-recovery point:

**Definition 3** (Recovery Half-Life)**.** *$\tau_{1/2}(t)$ is the minimum elapsed time after perturbation onset $t_{pert}$ at which the system's distance from the estimated attractor center $\mathbf{x}^*$ has decreased to half its post-perturbation value.*

In the biological context, increasing $\tau_{1/2}$ over successive episodes signals that the system is approaching a critical transition — it takes progressively longer to recover because its basin of attraction is shrinking [Scheffer et al., 2012]. This has been documented in cardiac systems, where increasing recovery times after exercise predict subsequent cardiac events [Scheffer et al., 2009]. At the cellular level, Benfatto et al. [2019] identified crucial events — abrupt, criticality-generated transitions — in biophoton emission from germinating seeds, showing that biological systems spontaneously generate the self-organized temporal criticality that our recovery half-life operator is designed to detect.

### 2.4 Variability Stabilization

Variability stabilization measures how quickly the system's variability structure (not just its mean) returns to baseline after perturbation.

**Definition 4** (Variability Stabilization)**.**

$$VS(t) = \frac{\|\Sigma(t) - \Sigma_0\|_F}{\|\Sigma(t_{pert}) - \Sigma_0\|_F} \tag{3}$$

*where $\Sigma(t)$ is the covariance matrix estimated over a window centered at $t$, $\Sigma_0$ is the baseline covariance, and $\|\cdot\|_F$ is the Frobenius norm.*

This signature captures a subtlety that mean-based recovery measures miss. A system can recover its mean values while its variability structure remains disturbed. In cardiac physiology, this manifests as normal mean heart rate with reduced HRV — a well-documented predictor of adverse outcomes [Task Force of the European Society of Cardiology and the North American Society of

Pacing and Electrophysiology, 1996, Buchman et al., 2002]. Multiscale entropy analysis [Costa et al., 2002, 2005] provides a rigorous framework for quantifying such variability structure across temporal scales, demonstrating that healthy physiological dynamics exhibit higher complexity than pathological ones at coarse time scales — precisely the kind of variability stabilization our VS signature measures. The Bounded Distortion operator $B(t)$ from the Coherence Engine measures a related quantity: whether the system's distortion (eigenvalue spread) remains within historical bounds.

### 2.5 Repeatability Across Episodes

Repeatability measures whether the system responds consistently to similar perturbations across episodes.

**Definition 5** (Episode Repeatability)**.** *For $K$ perturbation episodes with similar magnitude, the repeatability is:*

$$ER(t) = 1 - CV\left(\{\tau_{1/2}^{(k)}\}_{k=1}^{K}\right) = 1 - \frac{\sigma(\tau_{1/2})}{\mu(\tau_{1/2})} \tag{4}$$

*where CV is the coefficient of variation of recovery half-lives across episodes.*

High repeatability (ER $\to 1$) indicates a system with stable recovery dynamics. Declining repeatability indicates that the system's response to perturbation is becoming erratic — a qualitatively different degradation mode from simple slowing. A heart that sometimes recovers in 5 minutes and sometimes in 45 minutes after identical exercise bouts has lost repeatability even if its mean recovery time is unchanged.

### 2.6 Adaptive Response Quality

Adaptive response quality measures whether the system *improves* its recovery dynamics in response to repeated perturbations — the hallmark of healthy biological adaptation.

**Definition 6** (Adaptive Response Quality)**.**

$$AQ(t) = -\frac{d}{dt}\left[\mathbb{E}[\tau_{1/2}(t)]\right] \cdot \frac{1}{\tau_{1/2}(t_0)} \tag{5}$$

*where the expectation is over recent perturbation episodes. $AQ > 0$ indicates the system is adapting (recovery is speeding up); $AQ = 0$ indicates stasis; $AQ < 0$ indicates maladaptation (recovery is slowing despite repeated exposure).*

This is the signature most specific to biology. Engineered systems do not improve through use; biological systems should. A training program that improves cardiovascular fitness produces measurably faster recovery dynamics over weeks. A system that fails to adapt — or that maladapts, showing worsening recovery despite continued training — has lost a fundamental property of biological coherence. Figure 4 illustrates this divergence: over four perturbation episodes, a healthy system shows decreasing BD peaks and improving $\tau_{1/2}$, while a degrading system shows the opposite trajectory.

## 3 Distinguishing True Recovery from Compensation

The central insight of coherence-based biological assessment is that *return to baseline statistics does not imply recovery.* Two systems can exhibit identical resting values while having fundamentally different recovery dynamics. We formalize this distinction.

| Signature | Measures | Operator | Healthy |
|---|---|---|---|
| Baseline deviation (BD) | Distance from baseline | Drift $D(t)$ | Low, stable |
| Post-perturbation persistence (PP) | Duration of effects | Memory $M(t)$ | Short, consistent |
| Recovery half-life ($\tau_{1/2}$) | Recovery speed | Recovery $W(t)$ | Fast, stable |
| Variability stabilization (VS) | Covariance recovery | Distortion $B(t)$ | Fast return to $\Sigma_0$ |
| Episode repeatability (ER) | Cross-episode consistency | Pattern $P(t)$ | High ($\to 1$) |
| Adaptive response quality (AQ) | Improvement over time | (Biological) | Positive |

Table 1: Six biological recovery signatures, their measurement targets, corresponding Coherence Engine operators from [Thorarinson and Hensgen, 2026a], and healthy reference values.

**Definition 7** (True Recovery)**.** *A system has truly recovered from a perturbation at time $t$ if all six recovery signatures return to within one standard deviation of their baseline values:*

$$\textit{Recovered}(t) \iff \forall\, s \in \{BD, PP, \tau_{1/2}, VS, ER, AQ\} : \frac{|s(t) - s(t_0)|}{\sigma_s} \leq 1 \tag{6}$$

**Definition 8** (Compensation)**.** *A system is compensating if its output values have returned to baseline but its recovery signatures have not:*

$$\textit{Compensating}(t) \iff \|\mathbf{x}(t) - \mathbf{x}^*\| \leq \epsilon \quad \wedge \quad \exists\, s : \frac{|s(t) - s(t_0)|}{\sigma_s} > 1 \tag{7}$$

Consider two hearts, both resting at 72 bpm:

**Heart A** (recovered): After a 30-minute run, heart rate peaks at 160 bpm, then returns to 72 bpm in 8 minutes. HRV returns to baseline within 15 minutes. The recovery trajectory is smooth, monotonic, and consistent with previous exercise episodes. All six recovery signatures are within baseline range.

**Heart B** (compensating): After an identical run, heart rate also returns to 72 bpm — but it takes 22 minutes. HRV does not return to baseline for 4 hours. The recovery trajectory shows oscillations and overshoots. The mean endpoint is the same; the dynamics are different. BD is elevated, $\tau_{1/2}$ has doubled, VS shows persistent covariance disturbance, and ER is low because each exercise episode produces a different recovery pattern.

A threshold-based clinical system sees two identical hearts at 72 bpm. A coherence-based system sees one recovered heart and one compensating heart (Figure 1). This is the same distinction that the Coherence Engine detects in engines [Thorarinson and Hensgen, 2026a]: two engines can show similar mean sensor values while one has maintained its internal coordination and the other has lost it.

Scheffer et al. [2009] identified critical slowing down — increasing recovery time before a transition — as a universal early warning signal. Our framework extends this observation: critical slowing down is one of six signatures. A system can also lose coherence through decreased repeatability (ER), persistent post-perturbation effects (PP), or failure to adapt (AQ), each representing a different mode of recovery degradation.

Biophoton research provides supporting evidence for this multi-signature perspective. Wang et al. [2023] demonstrated that biophotonic activity induced by glutamate is significantly reduced and spectrally blue-shifted in both Alzheimer's disease and vascular dementia animal models, with these changes partially reversible through NMDAR antagonism — coherence degradation measured at the photon level, not merely at a clinical threshold. Racine et al. [2013] showed through Fano factor analysis and second-order correlation $g^{(2)}(0)$ measurements that biophoton signals from human hands exhibit quantum characteristics, suggesting that biological coherence may be measurable at the single-photon level. These findings support, though do not yet confirm, the proposition that coherence degradation is a fundamental feature of biological dysfunction detectable across measurement scales.

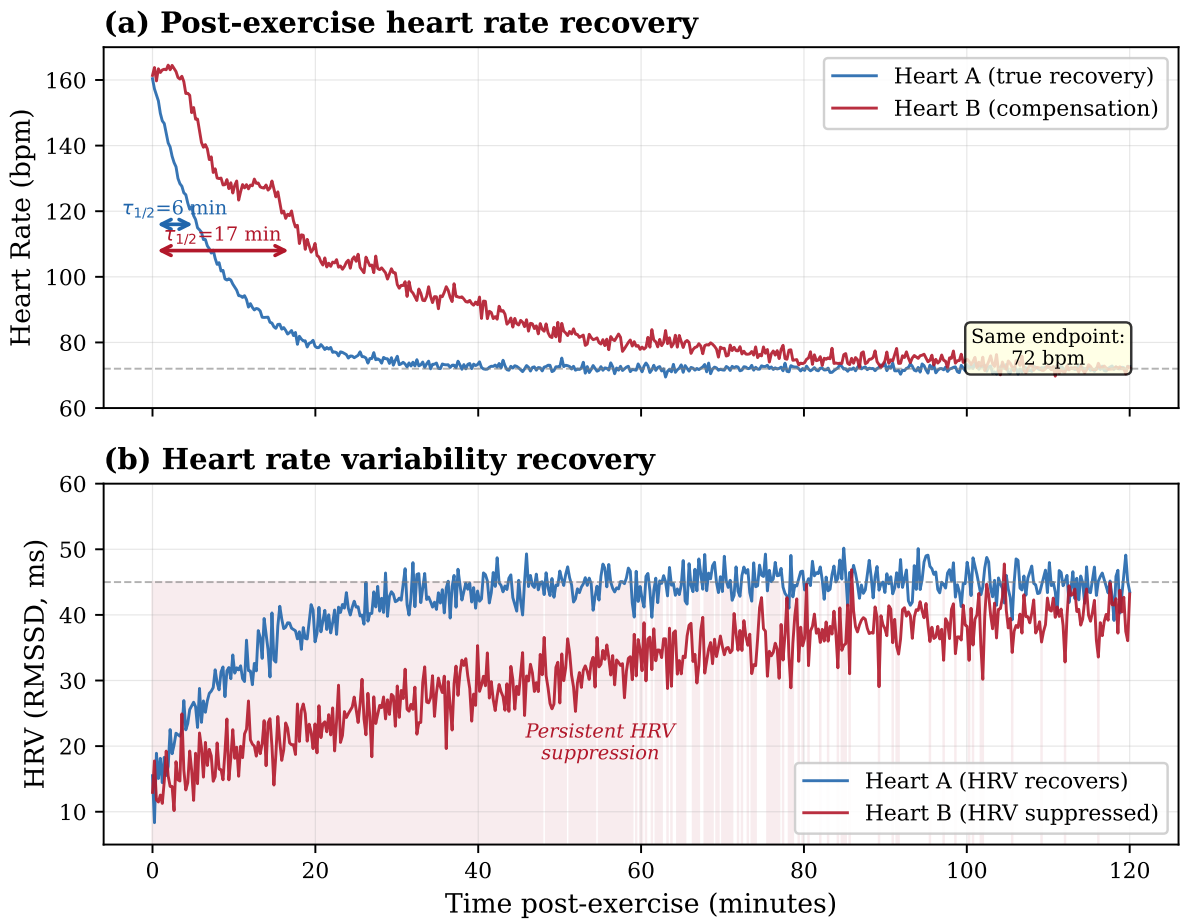


Figure 1: True recovery versus compensation. Both hearts return to 72 bpm, but Heart A recovers in 6 minutes with rapid HRV restoration, while Heart B takes 17 minutes with persistent HRV suppression lasting over an hour. The endpoint is identical; the recovery signatures are not. Simulated data with physiologically realistic parameters.

# 4 Application Domains

For each domain, we describe the perturbation protocol, recovery signature computation, data sources, and a specific testable prediction that could be validated with existing public datasets or standard clinical protocols.

## 4.1 Cardiac Recovery: Heart Rate Variability Post-Exercise

Heart rate variability (HRV) is the gold standard for autonomic nervous system assessment [Task Force of the European Society of Cardiology and the North American Society of Pacing and Electrophysiology, 1996, Shaffer and Ginsberg, 2017]. Post-exercise HRV recovery has been shown to predict cardiovascular events, training adaptation, and overtraining syndrome [Halson, 2014]. The fractal scaling properties of heart rate time series, quantified by detrended fluctuation analysis [Peng et al., 1995], provide a natural baseline against which recovery dynamics can be measured: healthy hearts exhibit long-range correlations with a scaling exponent $\alpha \approx 1.0$, while pathological states produce either random ($\alpha \approx 0.5$) or overly correlated ($\alpha > 1.0$) dynamics [Goldberger et al., 2002, Stanley et al., 1999].

**Perturbation protocol**: Standardized exercise bout (e.g., 20 minutes at 70% maximum heart rate).

**Recovery signatures**: (i) BD: Fisher-Rao distance of RR-interval distribution from resting baseline. (ii) PP: Time until HRV spectral features return to within 10% of baseline. (iii) $\tau_{1/2}$: Time for heart rate to return halfway from peak to resting. (iv) VS: Time for the HF/LF power ratio to stabilize. (v) ER: Coefficient of variation of $\tau_{1/2}$ across exercise sessions over a 4-week period. (vi) AQ: Trend in $\tau_{1/2}$ over the training program (should decrease with fitness gains).

**Data sources**: Optical PPG from Apple Watch (sampling at 1 Hz during recovery), chest-strap heart rate monitors (sampling at beat-to-beat resolution), clinical Holter monitors. Figure 2 demonstrates the full six-operator decomposition applied to a simulated 24-hour RR-interval series with three exercise perturbations, showing how each signature captures a different aspect of the recovery dynamics.

**Clinical relevance**: Declining ER and increasing $\tau_{1/2}$ over a training cycle are early indicators of overtraining syndrome, detectable before performance metrics decline or subjective fatigue is reported [Halson, 2014]. In critical care settings, loss of HRV complexity is among the earliest indicators of physiological decompensation [Buchman et al., 2002].

**Testable prediction**: In the MIT-BIH Arrhythmia Database [Moody and Mark, 2001] (PhysioNet ID: `mitdb`, 48 half-hour recordings, 360 Hz), patients with documented arrhythmias will exhibit lower episode repeatability (ER) in post-ectopic-beat recovery dynamics than normal sinus rhythm segments from the same recordings, even when mean RR-interval statistics are matched.

### 4.2 Metabolic Recovery: Glucose Response Curves

Continuous glucose monitors (CGMs) provide 5-minute resolution glucose data that captures the full dynamics of metabolic response and recovery [Rodbard, 2016].

**Perturbation protocol**: Standardized meal (e.g., 75g oral glucose tolerance test) or natural meals with estimated glycemic load.

**Recovery signatures**: (i) BD: Deviation of the 2-hour post-meal glucose curve from the individual's established response profile. (ii) PP: Time until glucose returns to within 10 mg/dL of pre-meal baseline. (iii) $\tau_{1/2}$: Time from glucose peak to half-return. (iv) VS: Variability of the recovery trajectory (smooth return vs. oscillatory "roller-coaster" pattern). (v) ER: Consistency of response to similar meals across days. (vi) AQ: Does repeated exposure to a food improve the glucose response? (Healthy adaptation: yes.)

**Clinical relevance**: Increasing PP and declining ER in glucose response curves may precede clinical pre-diabetes diagnosis by months to years. The trajectory *shape* contains information that fasting glucose and HbA1c miss.

**Testable prediction**: Among individuals with normal fasting glucose (<100 mg/dL) and normal HbA1c (<5.7%), those who subsequently develop pre-diabetes within 2 years will show measurably lower ER and longer PP in response to standardized oral glucose tolerance tests at baseline, compared to matched individuals who remain normoglycemic.

### 4.3 Neurological Recovery: EEG Post-Seizure Dynamics

Post-ictal EEG dynamics contain information about seizure severity, brain recovery capacity, and the risk of subsequent seizures.

**Dataset**: CHB-MIT Scalp EEG Database [Shoeb, 2010], available through PhysioNet [Goldberger et al., 2000] (PhysioNet ID: `chbmit`, 24 subjects, 198 seizures, 256 Hz sampling across 23 channels). EEG coherence and spectral analysis methods are well-established [Nunez and Srinivasan, 2006], and evidence of broadband criticality in brain network synchronization [Kitzbichler et al., 2009] suggests that recovery signatures should capture transitions between critical and subcritical dynamical regimes.

**Recovery signatures**: (i) BD: Fisher-Rao distance of post-ictal spectral distribution from inter-ictal baseline. (ii) PP: Duration of post-ictal suppression or abnormal spectral features.

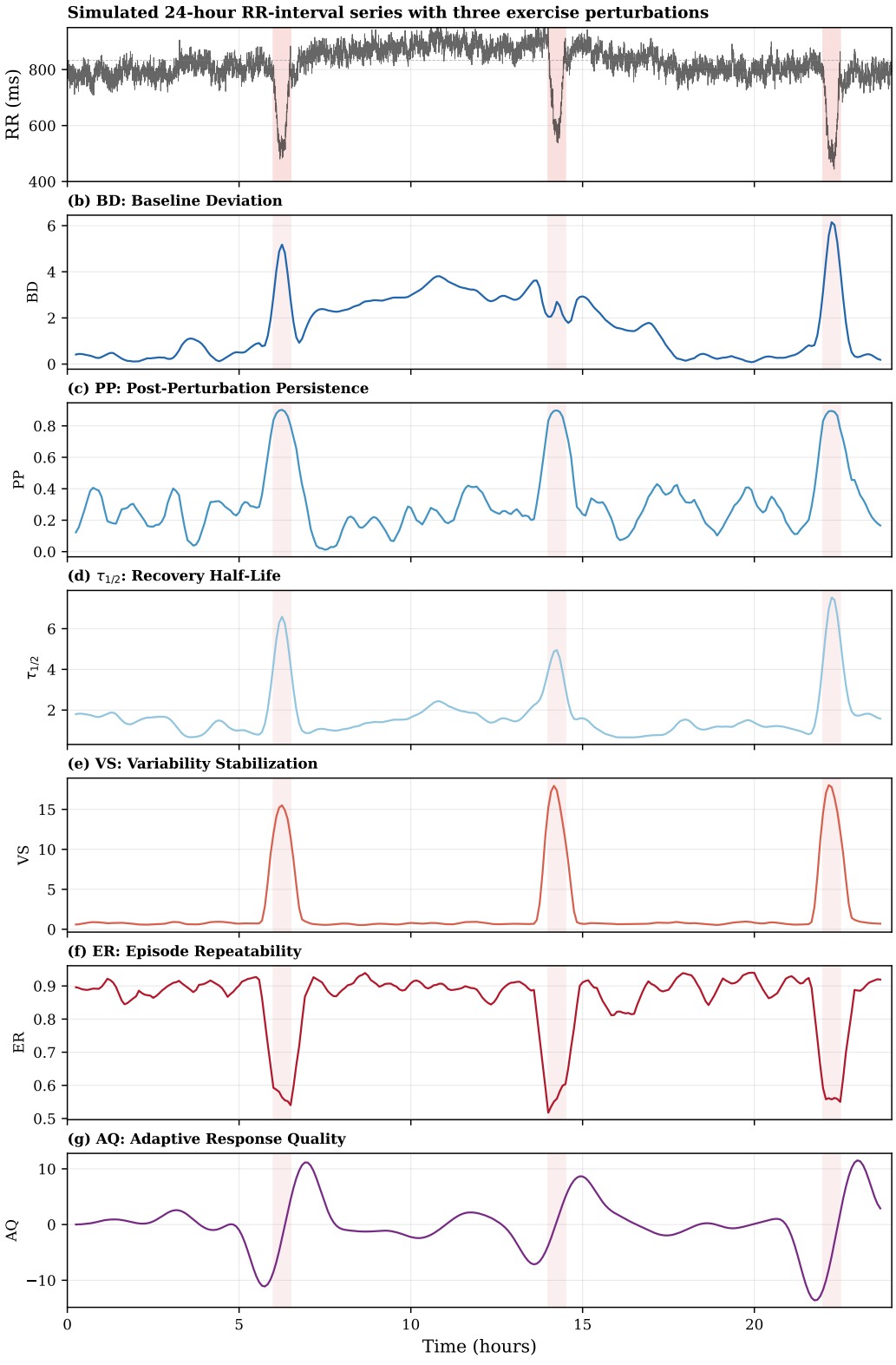


Figure 2: Coherence operator decomposition of a simulated 24-hour RR-interval time series with three exercise perturbations (shaded red). All six recovery signatures are computed over 30-minute rolling windows. BD and VS spike during exercise; PP captures persistence of perturbation effects; $\tau_{1/2}$ shows progressively slower recovery across episodes; ER drops during perturbations; AQ reflects the derivative of recovery dynamics. Simulated data with physiologically realistic parameters ($n = 86{,}400$ samples at 1 Hz).

(iii) $\tau_{1/2}$: Time for spectral coherence (measured as mean phase alignment $A(t)$ across channels) to return halfway to baseline. (iv) VS: Time for cross-channel correlation structure to stabilize. (v) ER: Consistency of post-ictal recovery across seizure episodes within the same patient. (vi) AQ: Do successive seizures produce worsening or improving recovery trajectories?

**Clinical relevance**: The Coherence Engine detected pre-seizure EEG desynchronization 687 seconds (∼11 minutes) before clinical onset [Thorarinson and Hensgen, 2026a]. Post-seizure recovery signatures may predict inter-seizure interval and medication response.

**Testable prediction**: Within the CHB-MIT dataset, patients with shorter inter-seizure intervals (<4 hours) will exhibit longer post-ictal $\tau_{1/2}$ and lower VS (slower return of cross-channel covariance to baseline) than patients with longer inter-seizure intervals (>24 hours), consistent with reduced recovery capacity preceding seizure recurrence.

### 4.4 Immune Response: Inflammatory Marker Trajectories

The immune system's response to infection or vaccination follows a perturbation–recovery arc that can be characterized by coherence signatures.

**Perturbation protocol**: Vaccination (standardized, controlled immune challenge) or tracked infection episodes.

**Recovery signatures**: (i) BD: Magnitude of inflammatory response (CRP, IL-6, TNF-$\alpha$) relative to individual baseline [Pepys and Hirschfield, 2003]. (ii) PP: Duration of elevated inflammatory markers. (iii) $\tau_{1/2}$: Time for inflammatory markers to return halfway to baseline. (iv) VS: Whether inflammatory marker correlations return to baseline structure. (v) ER: Consistency of immune response across vaccinations or infections. (vi) AQ: Does the immune system "learn" to produce a faster, more targeted response? (This is the definition of immunological memory.)

**Data sources**: Serial blood draws (research context), or proxy measures from wearables (resting heart rate elevation as an inflammation proxy, skin temperature from Oura ring).

**Testable prediction**: Following influenza vaccination, individuals with positive AQ (faster CRP normalization after dose 2 than dose 1) will show higher seroconversion titers at 28 days than individuals with zero or negative AQ, independent of baseline antibody levels.

### 4.5 Sleep Architecture: Recovery After Disruption

Sleep architecture — the proportion and sequencing of sleep stages [Rechtschaffen and Kales, 1968] — is itself a recovery signature, representing the brain's overnight recovery process.

**Perturbation protocol**: Sleep deprivation (one night of restricted sleep), jet lag (timezone shift), or acute stress.

**Recovery signatures**: (i) BD: Deviation of sleep stage proportions from individual baseline (REM%, deep%, light%). (ii) PP: Number of nights until sleep architecture returns to baseline. (iii) $\tau_{1/2}$: Number of nights to reach halfway recovery. (iv) VS: Variability of sleep metrics across recovery nights. (v) ER: Consistency of recovery pattern across disruption episodes. (vi) AQ: Does repeated exposure to disruption (e.g., shift work) produce adaptation or maladaptation?

**Data sources**: Consumer sleep trackers (Oura, Apple Watch), clinical polysomnography, actigraphy.

**Testable prediction**: After a standardized 4-hour sleep restriction night, individuals with high ER (consistent recovery pattern across disruption episodes) will show faster restoration of slow-wave sleep percentage on the first recovery night than individuals with low ER, even when matched on total sleep time and subjective sleepiness scores.

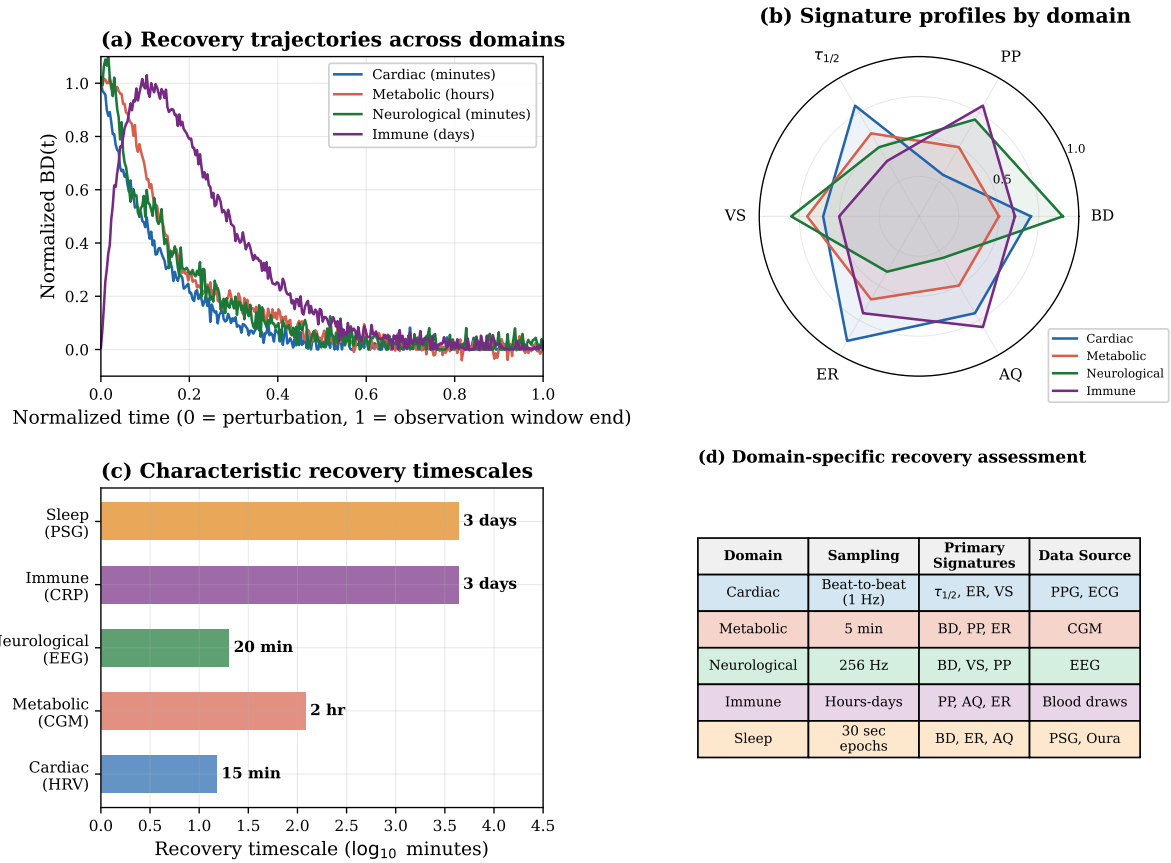


| Domain | Sampling | Primary Signatures | Data Source |
|---|---|---|---|
| Cardiac | Beat-to-beat (1 Hz) | $\tau_{1/2}$, ER, VS | PPG, ECG |
| Metabolic | 5 min | BD, PP, ER | CGM |
| Neurological | 256 Hz | BD, VS, PP | EEG |
| Immune | Hours-days | PP, AQ, ER | Blood draws |
| Sleep | 30 sec epochs | BD, ER, AQ | PSG, Oura |

Figure 3: Cross-domain recovery signature comparison. (a) Normalized recovery trajectories show domain-specific dynamics: cardiac recovery is fastest, immune response shows a delayed peak, and metabolic response exhibits characteristic oscillations. (b) Radar plots of signature profiles reveal that each domain emphasizes different aspects of recovery. (c) Characteristic timescales span four orders of magnitude. (d) Summary of domain-specific sampling requirements and primary signatures. Simulated data based on characteristic timescales from the literature; no experimental data are shown.

# 5 Wearable Data Pipeline

A practical pipeline for computing recovery signatures from consumer wearable data must address four challenges: sampling rate limitations, missing data, individual baseline estimation, and perturbation identification. Li et al. [2017] demonstrated that wearable biosensors can detect clinically meaningful physiological changes using continuous multi-modal monitoring, and the V3 validation framework [Goldsack et al., 2020] establishes standards for biometric monitoring technologies directly applicable to recovery signature computation.

## 5.1 Sampling Requirements

## 5.2 Pipeline Architecture

The pipeline operates in five stages:

1. **Baseline estimation**: Compute individual baseline statistics from a 14-day baseline period with no known perturbations. Estimate $p_0$, $\Sigma_0$, and $\tau_{1/2}^{(0)}$ from this period. Update baseline using exponential moving average with $\alpha = 0.01$ to account for healthy drift (aging, seasonal variation).

| Domain | Device | Sampling Rate | Minimum Window |
|---|---|---|---|
| Cardiac HRV | Apple Watch / chest strap | 1 Hz / beat-to-beat | 5 min (short-term HRV) |
| Glucose | CGM (Libre, Dexcom) | 1/300 Hz (5 min) | 2 hr (meal response) |
| Sleep | Oura / Apple Watch | 1/30 Hz (30 sec epochs) | 1 night (full architecture) |
| Activity | Accelerometer | 50 Hz (raw) / 1 min (processed) | 30 min (exercise bout) |
| Temperature | Oura / continuous | 1/60 Hz (1 min) | 24 hr (circadian) |

Table 2: Sampling rates and minimum window durations for recovery signature computation from consumer wearable devices.

2. **Perturbation detection**: Identify perturbation events automatically (exercise bouts from heart rate and accelerometry, meals from glucose spikes, sleep disruptions from actigraphy) or from user annotations.

3. **Recovery window extraction**: For each perturbation, extract the recovery window from perturbation end to either baseline return or the next perturbation, whichever comes first.

4. **Signature computation**: Compute all six recovery signatures for each recovery window. Store as a time-indexed record: (perturbation type, magnitude, BD, PP, $\tau_{1/2}$, VS, ER, AQ).

5. **Trend analysis**: Fit trends to each signature over rolling 28-day windows. Alert when any signature shows statistically significant degradation (two-sided $t$-test, $p < 0.01$, Bonferroni-corrected for six comparisons).

### 5.3 Individual Variation and Normalization

Biological recovery signatures vary enormously between individuals. A resting heart rate of 50 bpm is healthy for an athlete and concerning for a sedentary individual. The framework addresses this by measuring *within-individual change* rather than population-referenced thresholds. Each individual serves as their own baseline, and the signatures measure deviation from that individual's established recovery dynamics.

This is mathematically analogous to the Coherence Engine's use of a baseline period for each engine [Thorarinson and Hensgen, 2026a]: the question is not "is this engine's coherence score high or low?" but "is this engine's coherence score declining relative to its own baseline?"

## 6 Experimental Framework

We propose a framework for designing perturbation studies that directly measure biological coherence, rather than inferring it from observational data.

### 6.1 Controlled Perturbation Design

A coherence-measuring perturbation study has three phases:

1. **Baseline phase** (14–28 days): Continuous monitoring with no deliberate perturbations. Establish individual baselines for all six recovery signatures.

2. **Perturbation phase** (28–56 days): Administer standardized perturbations at regular intervals (e.g., exercise tests every 3 days, standardized meals daily). Compute recovery signatures after each perturbation. Monitor for trends.

3. **Intervention phase** (28–56 days): Introduce an intervention (medication change, training program modification, dietary change) and continue perturbation testing. Compare recovery signatures pre- and post-intervention.

The key design principle is that the perturbation is the *measurement instrument*, not the intervention. The perturbation reveals the system's recovery capacity; the intervention changes it. This is analogous to stress testing in cardiology (exercise reveals cardiac reserve) and in engineering (load testing reveals structural capacity).

### 6.2 Power Analysis

Recovery signatures are inherently higher-variance than static biomarkers because they measure dynamic processes. Power analysis for coherence studies must account for:

- Within-individual variation across perturbation episodes (ER provides a direct estimate)
- The minimum number of perturbation episodes needed to estimate $\tau_{1/2}$ with acceptable precision (typically $K \geq 5$ episodes)
- The effect size expected from the intervention on each signature

As a heuristic, detecting a 20% change in $\tau_{1/2}$ with power 0.80 and $\alpha = 0.05$ requires approximately 10 perturbation episodes per phase (baseline and intervention), given typical within-individual CVs of 15–25% for cardiac recovery metrics.

## 7 Limitations

Biological coherence measurement faces challenges that do not arise in engineered systems:

**Noise and confounders**: Biological time series are affected by circadian rhythms, meals, stress, sleep quality, hydration, medication timing, and dozens of other factors. Isolating the signal of recovery dynamics from these confounders requires either controlled laboratory conditions (limiting ecological validity) or sophisticated deconfounding methods (limiting certainty).

**Individual variation**: The normal range of recovery dynamics spans an order of magnitude across individuals. Population-level benchmarks are therefore limited; the framework's strength is within-individual tracking, which requires a longitudinal baseline period.

**Non-stationarity**: Healthy biological systems change over time (aging, training adaptation, seasonal variation). Distinguishing pathological drift from healthy non-stationarity is the fundamental challenge. The framework addresses this through slow baseline updating ($\alpha = 0.01$), but edge cases (rapid healthy adaptation, such as during early training) may produce false alarms.

**Wearable data quality**: Consumer wearable devices have lower sampling rates, more missing data, and less accuracy than clinical instruments [Goldsack et al., 2020]. Recovery signatures computed from wearable data will have wider confidence intervals than those from clinical-grade monitoring. The framework is designed to be robust to this by operating on distributional features (Fisher-Rao distance, covariance structure) rather than point estimates.

**No experimental validation yet**: This paper proposes and motivates a framework; it does not validate it empirically. The recovery signatures are formalized mathematically and grounded in existing physiological and biophoton literature, but their predictive value in each application domain remains to be tested. The testable predictions in Section 4 are designed to enable such validation using publicly available datasets and standard clinical protocols.

**Ethical considerations**: Continuous health monitoring raises concerns about data privacy, anxiety induction (false alarms about health status), and the medicalization of everyday variation. A coherence-based system that alerts a user to "declining recovery dynamics" must be carefully calibrated to avoid producing harmful anxiety from clinically meaningless fluctuations.

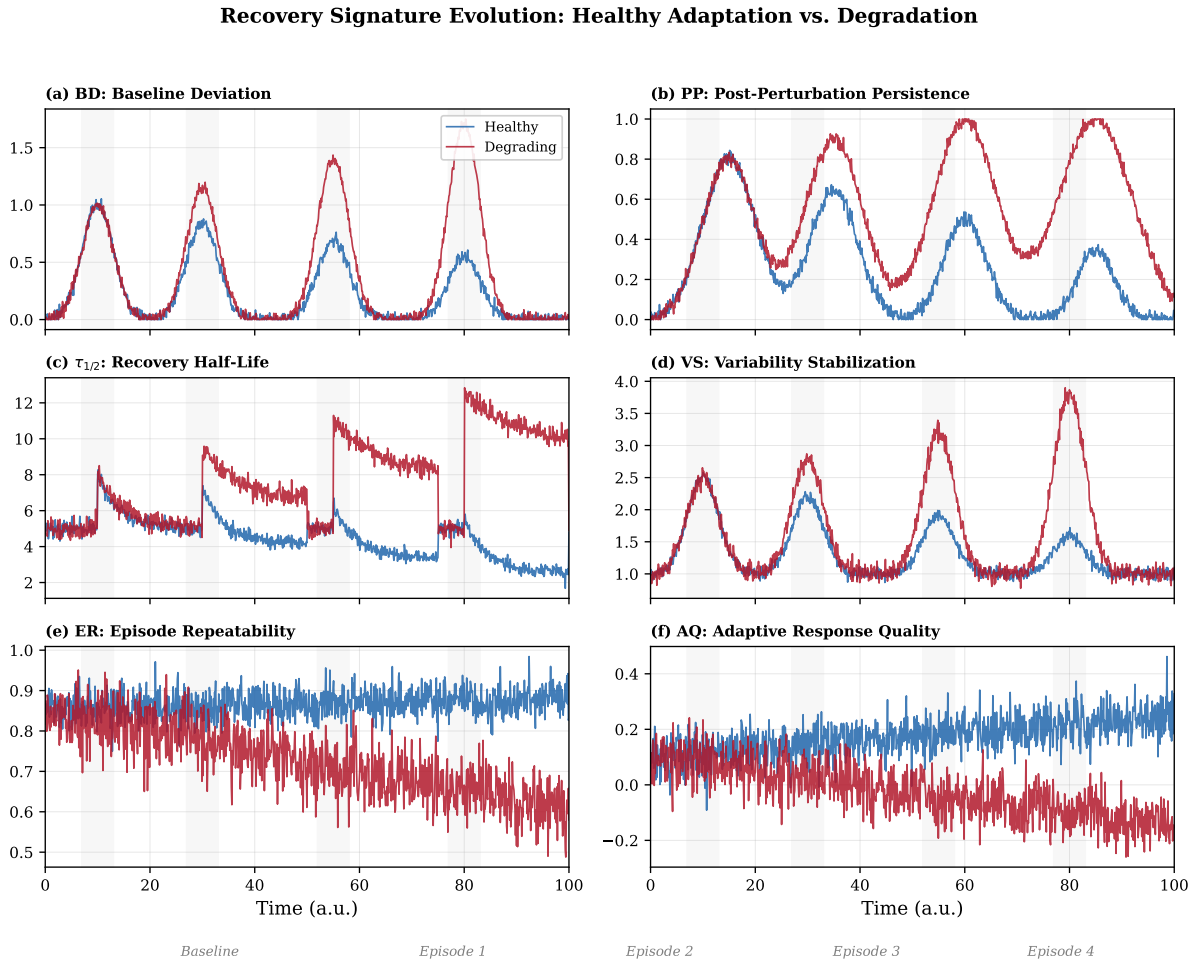


Figure 4: Recovery signature evolution over four perturbation episodes, comparing a healthy system (blue) that adapts over time with a degrading system (red) that maladapts. The healthy system shows decreasing BD peaks, shortening $\tau_{1/2}$, stable ER, and positive AQ. The degrading system shows increasing BD peaks, lengthening $\tau_{1/2}$, declining ER, and negative AQ. Gray shading marks perturbation periods. Simulated data.

# 8 Conclusion

Recovery is not return to baseline. Recovery is return to coherent function — the capacity to respond to perturbation, return to equilibrium, and do so consistently and adaptively across episodes. A system that returns to the same resting values but takes twice as long, does so inconsistently, and fails to improve over time has not recovered, regardless of what its static biomarkers say.

The six biological recovery signatures defined here — baseline deviation, post-perturbation persistence, recovery half-life, variability stabilization, episode repeatability, and adaptive response quality — provide a continuous, quantitative framework for assessing this capacity. Grounded in the Coherence Engine operators [Thorarinson and Hensgen, 2026a] and adapted to biological data, these signatures target the dimension of health that threshold-based clinical assessment misses: the quality of the system's dynamic response, not just its resting state.

The framework is translational in nature: it takes operators validated on engineered systems (where ground truth failure data exist) and proposes their adaptation to biological measurement (where the same mathematical structure applies but compensation dynamics add complexity). The embedding coherence work of Thorarinson and Hensgen [2026b] established this principle

in information spaces; here we propose and motivate it in physiological spaces. As De Paolis et al. [2024] note, the fundamental question of whether biophotonic emission arises from random radiative decay or from a coherent electromagnetic field remains unresolved. Our framework does not require resolving this question — it measures coherence in the emitted signal regardless of the underlying mechanism.

The practical implication, pending empirical validation of the testable predictions in Section 4, is a new layer of health assessment: beneath the binary thresholds of clinical practice, a continuous measurement of the system's recovery integrity. Not "is your heart rate normal?" but "is your heart's capacity for coherent recovery intact?" The first question has a binary answer. The second has a trajectory — and the trajectory is where the early warning lives.

## References


Shun-ichi Amari. *Information Geometry and Its Applications*. Springer, 2016.

Maurizio Benfatto, Elisabetta Pace, Catalina Curceanu, Alessandro Scordo, Alberto Clozza, Ivan Davoli, Massimiliano Lucci, Roberto Francini, Fabio De Matteis, Maurizio Grandi, Rohisha Tuladhar, and Paolo Grigolini. Biophotons: Low signal/noise ratio reveals crucial events. *bioRxiv*, 2019. doi: 10.1101/558353.

Maurizio Benfatto, Elisabetta Pace, Catalina Curceanu, Alessandro Scordo, Alberto Clozza, Ivan Davoli, Massimiliano Lucci, Roberto Francini, Fabio De Matteis, Maurizio Grandi, Rohisha Tuladhar, and Paolo Grigolini. Biophotons and emergence of quantum coherence—a diffusion entropy analysis. *Entropy*, 23(5):554, 2021. doi: 10.3390/e23050554.

Maurizio Benfatto, Elisabetta Pace, Ivan Davoli, Roberto Francini, Fabio De Matteis, Alessandro Scordo, Alberto Clozza, Luca De Paolis, Catalina Curceanu, and Paolo Grigolini. Biophotons: New experimental data and analysis. *Entropy*, 25(10):1431, 2023. doi: 10.3390/e25101431.

Christian Brouder and Michal Cifra. Coherence and statistical properties of ultra-weak photon emission. In Daniel Fels, Michal Cifra, and Felix Scholkmann, editors, *Fields of the Cell*, pages 163–188. Research Signpost, 2015. ISBN 978-81-308-0544-3.

Timothy G Buchman, Phyllis K Stein, and Bruce Goldstein. Heart rate variability in critical illness and critical care. *Current Opinion in Critical Care*, 8(4):311–315, 2002. doi: 10.1097/00075198-200208000-00007.

Madalena Costa, Ary L Goldberger, and C-K Peng. Multiscale entropy analysis of complex physiologic time series. *Physical Review Letters*, 89(6):068102, 2002. doi: 10.1103/PhysRevLett.89.068102.

Madalena Costa, Ary L Goldberger, and C-K Peng. Multiscale entropy analysis of biological signals. *Physical Review E*, 71(2):021906, 2005. doi: 10.1103/PhysRevE.71.021906.

Vasilis Dakos, Stephen R Carpenter, William A Brock, Aaron M Ellison, Vishwesha Guttal, Anthony R Ives, Sonia Kéfi, Valerie Livina, David A Seekell, Egbert H van Nes, and Marten Scheffer. Methods for detecting early warnings of critical transitions in time series illustrated using simulated ecological data. *PloS One*, 7(7):e41010, 2012.

Luca De Paolis, Roberto Francini, Ivan Davoli, Fabio De Matteis, Alessandro Scordo, Alberto Clozza, Maurizio Grandi, Elisabetta Pace, Catalina Curceanu, Paolo Grigolini, and Maurizio Benfatto. Biophotons: A hard problem. *Applied Sciences*, 14(13):5496, 2024. doi: 10.3390/app14135496.

Martin Dlask, Jaromír Kukal, Michaela Poplová, Pavel Sovka, and Michal Cifra. Short-time fractal analysis of biological autoluminescence. *bioRxiv*, 2019. doi: 10.1101/578286.

Ary L Goldberger, Luís A N Amaral, Leon Glass, Jeffrey M Hausdorff, Plamen Ch Ivanov, Roger G Mark, Joseph E Mietus, George B Moody, C-K Peng, and H Eugene Stanley. PhysioBank, PhysioToolkit, and PhysioNet: Components of a new research resource for complex physiologic signals. *Circulation*, 101(23):e215–e220, 2000. doi: 10.1161/01.CIR.101.23.e215.

Ary L Goldberger, Luís A N Amaral, Jeffrey M Hausdorff, Plamen Ch Ivanov, C-K Peng, and H Eugene Stanley. Fractal dynamics in physiology: Alterations with disease and aging. *Proceedings of the National Academy of Sciences*, 99(Suppl 1):2466–2472, 2002. doi: 10.1073/pnas.012579499.

Jennifer C Goldsack, Andrea Coravos, Jessie P Bakker, Brinnae Bent, Ariel V Dowling, Cheryl Fitzer-Attas, Alan Godfrey, Job G Godino, Nikhil Guber, Conor Heneghan, et al. Verification, analytical validation, and clinical validation (V3): The foundation of determining fit-for-purpose for biometric monitoring technologies (BioMeTs). *npj Digital Medicine*, 3:55, 2020. doi: 10.1038/s41746-020-0260-4.

Shona L Halson. Monitoring training load to understand fatigue in athletes. *Sports Medicine*, 44 (Suppl 2):S139–S147, 2014. doi: 10.1007/s40279-014-0253-z.

Manfred G Kitzbichler, Marie L Smith, Sren R Christensen, and Ed Bullmore. Broadband criticality of human brain network synchronization. *PLoS Computational Biology*, 5(3):e1000314, 2009. doi: 10.1371/journal.pcbi.1000314.

Timothy M Lenton. Early warning of climate tipping points. *Nature Climate Change*, 1(4): 201–209, 2011.

Xiao Li, Jessilyn Dunn, Denis Salins, Gao Zhou, Wenyu Zhou, Sophia M Schüssler-Fiorenza Rose, Dalia Perelman, Elizabeth Colbert, Ryan Runge, Shannon Rego, et al. Digital health: Tracking physiomes and activity using wearable biosensors reveals useful health-related information. *PLoS Biology*, 15(1):e2001402, 2017. doi: 10.1371/journal.pbio.2001402.

Lewis A Lipsitz and Ary L Goldberger. Loss of "complexity" and aging: Potential applications of fractals and chaos theory to senescence. *JAMA*, 267(13):1806–1809, 1992.

Bruce S McEwen. Protective and damaging effects of stress mediators. *New England Journal of Medicine*, 338(3):171–179, 1998. doi: 10.1056/NEJM199801153380307.

Bruce S McEwen. Protection and damage from acute and chronic stress: Allostasis and allostatic overload and relevance to the pathophysiology of psychiatric disorders. *Annals of the New York Academy of Sciences*, 1032(1):1–7, 2004. doi: 10.1196/annals.1314.001.

George B Moody and Roger G Mark. The impact of the MIT-BIH arrhythmia database. *IEEE Engineering in Medicine and Biology Magazine*, 20(3):45–50, 2001.

Paul L Nunez and Ramesh Srinivasan. *Electric Fields of the Brain: The Neurophysics of EEG*. Oxford University Press, 2 edition, 2006.

C-K Peng, Shlomo Havlin, H Eugene Stanley, and Ary L Goldberger. Quantification of scaling exponents and crossover phenomena in nonstationary heartbeat time series. *Chaos*, 5(1):82–87, 1995. doi: 10.1063/1.166141.

Mark B Pepys and Gideon M Hirschfield. C-reactive protein: A critical update. *Journal of Clinical Investigation*, 111(12):1805–1812, 2003. doi: 10.1172/JCI18921.

David Racine, Anshu Rastogi, and Rajendra P. Bhajpai. Hints at quantum characteristics of light signals measured from a human subject. *Chinese Medicine*, 4(3):72–78, 2013. doi: 10.4236/cm.2013.43011.

C Radhakrishna Rao. Information and the accuracy attainable in the estimation of statistical parameters. *Bulletin of the Calcutta Mathematical Society*, 37:81–91, 1945.

Allan Rechtschaffen and Anthony Kales. *A Manual of Standardized Terminology, Techniques and Scoring System for Sleep Stages of Human Subjects*. US Government Printing Office, Washington, DC, 1968.

David Rodbard. Continuous glucose monitoring: A review of successes, challenges, and opportunities. *Diabetes Technology & Therapeutics*, 18(Suppl 2):S3–S13, 2016. doi: 10.1089/dia.2015.0417.

Marten Scheffer, Jordi Bascompte, William A Brock, Victor Brovkin, Stephen R Carpenter, Vasilis Dakos, Hermann Held, Egbert H Van Nes, Max Rietkerk, and George Sugihara. Early-warning signals for critical transitions. *Nature*, 461(7260):53–59, 2009.

Marten Scheffer, Stephen R Carpenter, Timothy M Lenton, Jordi Bascompte, William Brock, Vasilis Dakos, Johan van de Koppel, Ingrid A van de Leemput, Simon A Levin, Egbert H van Nes, Mercedes Pascual, and John Vandermeer. Anticipating critical transitions. *Science*, 338 (6105):344–348, 2012. doi: 10.1126/science.1225244.

Fred Shaffer and J. P. Ginsberg. An overview of heart rate variability metrics and norms. *Frontiers in Public Health*, 5:258, 2017. doi: 10.3389/fpubh.2017.00258.

Ali H Shoeb. *Application of Machine Learning to Epileptic Seizure Detection*. PhD thesis, Massachusetts Institute of Technology, 2010.

H Eugene Stanley, Luís A N Amaral, Ary L Goldberger, Shlomo Havlin, Plamen Ch Ivanov, and C-K Peng. Statistical physics and physiology: Monofractal and multifractal approaches. *Physica A: Statistical Mechanics and its Applications*, 270(1):309–324, 1999. doi: 10.1016/S0378-4371(99)00230-7.

Task Force of the European Society of Cardiology and the North American Society of Pacing and Electrophysiology. Heart rate variability: Standards of measurement, physiological interpretation, and clinical use. *Circulation*, 93(5):1043–1065, 1996. doi: 10.1161/01.CIR.93.5.1043.

Joel Thorarinson and Allison Hensgen. From prediction to discoverative intelligence: A coherence-based AI framework for detecting system drift before failure. *arXiv preprint*, 2026a.

Joel Thorarinson and Allison Hensgen. The dimensionality illusion: Why PCA variance does not equal semantic information in text embeddings. *arXiv preprint*, 2026b.

Zhuo Wang, Zhipeng Xu, Yi Luo, Sisi Peng, Hao Song, Tian Li, Jiaxin Zheng, Na Liu, Shenjia Wu, Junxia Zhang, Lei Zhang, Yuan Hu, Yanping Liu, Dongwei Lu, Jiapei Dai, and Junjian Zhang. Reduced biophotonic activities and spectral blueshift in Alzheimer's disease and vascular dementia models with cognitive impairment. *Frontiers in Aging Neuroscience*, 15: 1208274, 2023. doi: 10.3389/fnagi.2023.1208274.

Bruce J West. *Where Medicine Went Wrong: Rediscovering the Path to Complexity*. Studies of Nonlinear Phenomena in Life Science. World Scientific, 2006.